



Article

The Effect of Socioeconomic Factors on Spatiotemporal Patterns of PM_{2.5} Concentration in Beijing–Tianjin–Hebei Region and Surrounding Areas

Wenting Wang ^{1,2,3,†}, Lijun Zhang ^{2,†}, Jun Zhao ^{1,2}, Mengge Qi ^{1,2} and Fengrui Chen ^{1,2,*}

¹ Key Laboratory of Geospatial Technology for the Middle and Lower Yellow River Regions, Ministry of Education/Collaborative Innovation Center of Yellow River Civilization, Henan University, Kaifeng 475004, China; wangwentong@nsbd.cn (W.W.); ZhaoJun783783@126.com (J.Z.); qq491268037@outlook.com (M.Q.)

² College of Environmental and Planning, Henan University, Kaifeng 475004, China; zljhappy@163.com

³ South-to-North Water Diversion Middle Route Information Technology Co., Ltd., Beijing 100038, China

* Correspondence: frch@henu.edu.cn; Tel.: +86-371-2388-1850

† Both authors contributed equally to this work.

Received: 26 March 2020; Accepted: 24 April 2020; Published: 26 April 2020

Abstract: The study investigated the spatiotemporal evolution of PM_{2.5} concentration in the Beijing–Tianjin–Hebei region and surrounding areas during 2015–2017, and then analyzed its socioeconomic determinants. First, an estimation model considering spatiotemporal heterogeneous relationships was developed to accurately estimate the spatial distribution of PM_{2.5} concentration. Additionally, socioeconomic determinants of PM_{2.5} concentration were analyzed using a spatial panel Dubin model, which aimed to improve the robustness of the model estimation. The results demonstrated that: (1) The proposed model significantly increased the estimation accuracy of PM_{2.5} concentration. The mean absolute error and root-mean-square error were 9.21 µg/m³ and 13.10 µg/m³, respectively. (2) PM_{2.5} concentration in the study area exhibited significant spatiotemporal changes. Although the PM_{2.5} concentration has declined year by year, it still exceeded national environmental air quality standards. (3) The per capita GDP, urbanization rate and number of industrial enterprises above the designated size were the key factors affecting the spatiotemporal distribution of PM_{2.5} concentration. This study provided scientific references for comprehensive PM_{2.5} pollution control in the study area.

Keywords: PM_{2.5}; socioeconomic factors; spatiotemporal patterns; spatiotemporal heterogeneous; spatial panel Dubin model

1. Introduction

Atmospheric pollution significantly influences human health, climatic environment, and sustainable urban development [1–4]. According to a World Health Organization (WHO) report in 2014, atmospheric pollution causes more than seven million deaths worldwide each year [5]. A recent study based on the Global Exposure Mortality Model estimated that 8.9 million people died globally in 2015 [6]. With China's rapid economic, industrial, and urban development, atmospheric pollution has become an increasing problem. East China, especially the Beijing–Tianjin–Hebei region, has witnessed frequent occurrences of severe haze since 2013. The Beijing–Tianjin–Hebei region is responsible for the majority of North China's economic development, and coordinated development in this region is one of three national strategies in China [7]. Therefore, comprehensive atmospheric pollution governance in the region has attracted wide attention from China's government. PM_{2.5} (atmospheric particulate matter with a diameter of less than 2.5 µm) is the primary cause of haze.

Twenty-eight cities in the Beijing–Tianjin–Hebei region and surrounding areas are considered to be the main transmission channels of atmospheric pollution in the region. Hence, accurate interpretation of spatiotemporal distribution and evolution of PM_{2.5} concentrations in the Beijing–Tianjin–Hebei region and surrounding areas, as well as a recognition of the primary influencing factors of PM_{2.5} concentrations, have important theoretical and practical significance to atmospheric pollution control.

An accurate estimation of the spatial distribution of PM_{2.5} concentration is a prerequisite for determining its determinants. Traditionally, the spatial distribution of PM_{2.5} concentration is generated through spatially interpolating ground PM_{2.5} observations [8,9]. Although the ground observations are accurate, the observation stations are limited in number and distributed unevenly, thus making it difficult to produce accurate spatial distribution solely by interpolating the ground observations. Moreover, observations also suffer from a representativeness error. With the assistance of relevant auxiliary variables (e.g., satellite-derived Aerosol Optical Depth (AOD) data), the estimation accuracy of PM_{2.5} concentrations can be significantly improved. Various estimation models based on the relationship between PM_{2.5} and auxiliary variables have been proposed. These methods can be divided into two categories, i.e., physical models and statistical models. The physical models use atmospheric chemistry models to simulate the association between AOD and PM_{2.5}, and then estimate PM_{2.5} using satellite-derived AOD and the derived association [10–12]. The statistical models apply statistical methods (e.g., multiple linear regression, generalized additive model, and random forest) to investigate the relationship between ground-measured PM_{2.5} and satellite-derived AOD and other auxiliary variables, and then builds an estimation model based on the derived relationship [13–18]. Most of the statistical models argued that PM_{2.5} concentration is affected by the selected auxiliary variables that are fixed throughout the estimation period. However, it has been reported that PM_{2.5} is sensitive to meteorological conditions, but this sensitivity changes over time [19–21]. For example, certain meteorological factors may not significantly affect PM_{2.5} concentration during a specific period [22]. Additionally, AOD is an optical remote sensing product, which is significantly influenced by weather conditions (e.g., cloud and rain), resulting in a large amount of data gaps. All of these factors inevitably have adverse effects on accurately estimating the spatial distribution of PM_{2.5} concentration.

Determining factors that influence PM_{2.5} concentration have recently generated increased research interest and involves various aspects, including economic development, natural conditions, and urbanization [23–26]. Although such research can provide useful references for formulating atmospheric environmental governance policies, it still has some shortages. It is common to represent PM_{2.5} concentration of a region based on one ground measurement [23,27,28]. Due to significant spatial variation in PM_{2.5} concentration, such simplification will likely corrode the reliability of results. Although some studies have estimated PM_{2.5} concentration in urban areas based on gridded PM_{2.5} data [29,30], these grid data mainly come from interpolation of ground PM_{2.5} observation data or from statistical models based on satellite-derived AOD. Nevertheless, it was not until February 2012 that China measured PM_{2.5} concentration as a proxy for environmental air quality and at the end of 2014 a national observation network to measure PM_{2.5} levels was established (~1500 observation stations). Therefore, the interpolation results and statistical model results before 2014 may have larger uncertainty due to the limitation of available observations. The relationship between PM_{2.5} concentration and influencing factors are complicated, which creates some uncertainty in model construction. Some studies have focused on the relationship from a time-series perspective without regarding the spatial dependence of PM_{2.5} pollution [24,29,31]. Given the spatial dependence of atmospheric pollution, some studies applied spatial models to investigate the influencing factors on PM_{2.5} concentration [32,33]. However, the spatial model usually only considers panel data at a particular time, which may obtain different or even opposite results for panel data at different times because of the small sample data size. Although many studies have explored factors that influence PM_{2.5} concentration, it should be noted that at different stages of development, there can be substantial differences in economic growth, energy consumption, industrial structure, population,

and environmental background. Ignoring these differences is very likely to cause biased or suspicious conclusions.

Given that the national observation network was not completed until the end of 2014, this study focused on the spatiotemporal evolution of PM_{2.5} concentration in 28 cities of the Beijing–Tianjin–Hebei region and surrounding areas during 2015–2017, and then identified its socioeconomic determinants. Firstly, an estimation model for high spatial-resolution PM_{2.5} estimation was created based on the reconstructed AOD missing gaps and the spatiotemporal heterogeneous relationship between PM_{2.5} and auxiliary variables, which disclosed the spatial distribution of PM_{2.5} concentration in the study area. Secondly, based on the analysis of the spatiotemporal evolution of PM_{2.5} concentration, the socioeconomic factors that influence local PM_{2.5} concentration were investigated by a spatial panel model. The research study's conclusions provide scientific references for local atmospheric pollution control.

2. Study Area and Data

2.1. Study Area

The study area includes 28 cities of the Beijing–Tianjin–Hebei region and surrounding areas, covering an area of ~275,000 km². As shown in Figure 1, the terrain is high in the west and low in the east, with elevation ranging from sea level to >2000 m. The region experiences four distinct seasons, with hot and rainy summers due to the East Asian monsoon, and cold and dry winters due to subtropical high-pressure systems. The Beijing–Tianjin–Hebei region is the most economically developed area in northern China and is the area with the most PM_{2.5} pollution.

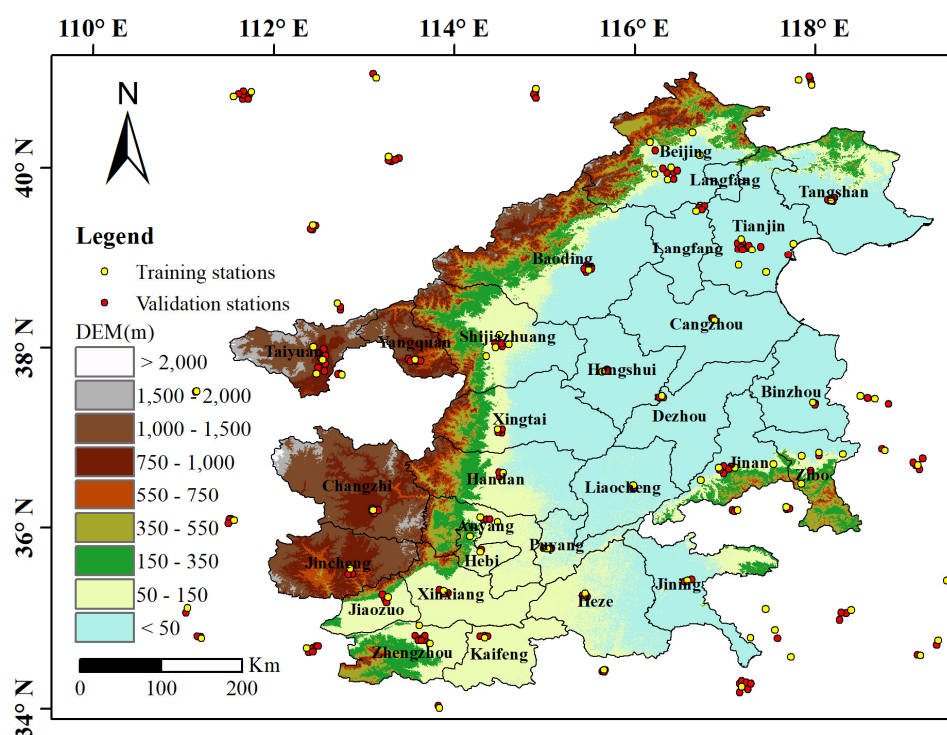


Figure 1. Study area and spatial distribution of ground PM 2.5 observation stations.

2.2. Data

Ground PM_{2.5} observations were from the public platform of the China National Environmental Monitoring Center (<http://www.cnemc.cn>). Before release, these data had been calibrated and quality controlled to meet the national environmental air quality standards of China (GB3095-2012). The present study used daily average PM_{2.5} concentration (DAPC) data from January 2015 to December 2017 at 256 observation stations in the study area and surrounding areas. Data of monthly average

PM_{2.5} concentrations (MAPC) were generated by averaging the DAPC. Spatial distribution of observation stations is shown in Figure 1. Among 256 observation stations, 83 were used for constructing the PM_{2.5} estimation model, and the remaining were used to verify the accuracy of the estimation results.

The latest C6 version of daily AOD (DAOD) was used to construct PM_{2.5} concentration estimation model. The C6 version DAOD had higher spatial resolutions (3 km) compared with the previous C5 version. Data of DAOD of Aqua (DAODA) and DAOD of Terra (DAODT) from January 2015 to December 2017 were collected from the website <https://ladsweb.modaps.eosdis.nasa.gov/>.

According to practical situations in the study area, air temperature (AT), wind speed (WS) at 10 m, surface pressure (SP), and boundary layer height (BLH) were chosen to assist the estimated spatial distribution of PM_{2.5} concentration (Table 1). These data came from the ERA-Interim reanalysis data (<http://apps.ecmwf.int/datasets/>) of the European Centre for Medium-Range Weather Forecast, with a spatial resolution of 0.125°.

Table 1. Definition of the variables used in the study.

Variable	Definition	Unit
AT	Air temperature at 2 m	K
WS	Wind speed at 10 m	m/s
BLH	Boundary layer height	m
SP	Surface pressure	Pa
PD	person density	person/km ²
PGRP	Per capital gross regional product	yuan
UR	Urbanization rate	%
PSIGDP	The proportion of secondary industry in GDP	%
ISDE	Industrial smoke (dust) emissions	ton/year
NIEDS	The number of industrial enterprises above designated size	unit

Socioeconomic data were collected from the China Statistics Yearbook, China City Statistics Yearbook and statistical yearbooks of provinces and regions in the study area (<http://data.cnki.net/Yearbook>). Six factors were chosen: person density (PD), per capita gross regional product (PGRP), urbanization rate (UR), the proportion of secondary industry in GDP (PSIGDP), industrial smoke (dust) emissions (ISDE), and the number of industrial enterprises above designated size (NIEDS) (Table 1). All PGRP data were transformed uniformly to a constant price in 2015. Additionally, logarithmic transformations were performed on all socioeconomic data to eliminate their heteroscedasticity.

3. Methodology

3.1. PM_{2.5} Estimation

Due to the impact of clouds, rain, and other weather conditions, there are a lot of gaps (no data region) in DAOD data. Therefore, it was necessary to fill the missing data gaps. DAOD data were constructed based on the complementarity between DAODT and DAODA on spatial coverage and significant correlation. The data were filled as follows:

DAODT and DAODA of a month were used to establish the relationship:

$$\text{DAODT}_m = a_{T,m} + b_{T,m} * \text{DAODA}_m + \varepsilon_T \quad (1)$$

$$\text{DAODA}_m = a_{A,m} + b_{A,m} * \text{DAODT}_m + \varepsilon_A \quad (2)$$

where m refers to month. $a_{T,m}$, $b_{T,m}$, $a_{A,m}$ and $b_{A,m}$ are regression coefficients between DAODT and DAODA. ε_T and ε_A are error terms.

Next, the missing data gaps of DAODT and DAODA were reconstructed based on the acquired relationships in Equations (1) and (2), generating reconstructed DAODT (RDAODT) and reconstructed DAODA (RDAODA). For example, if DAODT has a value V_{test} at location L_{test} , but DAODA does not, we can use V_{test} and Equation (2) to estimate the value of DAODA at location L_{test} . In this way, DAOD was estimated as $(\text{RDAODT} + \text{RDAODA})/2$ because Aqua and Terra measure AOD in the morning and afternoon, respectively. Finally, the monthly DAOD averages were calculated, which were used to generate the monthly average AOD data (MAOD).

Although AOD is an indicator of $\text{PM}_{2.5}$ concentration, $\text{PM}_{2.5}$ concentration is also significantly influenced by air temperature, precipitation, and other climatic factors [34,35]. This study used MAOD, AT, WS, BLH, and SP as the auxiliary variables to estimate the spatial distribution of $\text{PM}_{2.5}$ concentration. We assumed that the relationship between $\text{PM}_{2.5}$ concentration and auxiliary variables changes with time and space and the following model was constructed:

$$\widehat{\text{MAPC}}_m(u) = \alpha_m(u) + \beta_{m,0}(u) * \text{MAOD}_m(u) + \sum_{i=0}^n \beta_{m,i}(u) * \text{AUX}_{m,i}(u) \quad (3)$$

where $\widehat{\text{MAPC}}_m$ is the estimated average $\text{PM}_{2.5}$ concentration during the month m . u refers to spatial position. α_m is intercept, and $\beta_{m,0}$ and $\beta_{m,i}$ are coefficients of MAOD_m and other auxiliary variables $\text{AUX}_{m,i}$. n is a variable with a value range of ≤ 4 . When $n = 0$, no climatic factor is chosen. When $n = 4$, the AT, WS, BLH, and SP were all used to construct the model.

With regards to the temporal heterogeneous relationship between $\text{PM}_{2.5}$ and auxiliary variables, the auxiliary variables of the model were chosen based on the following criteria with consideration to temporal changes of the relationship between $\text{PM}_{2.5}$ and auxiliary variables: (1) the chosen auxiliary variables were significantly correlated with $\text{PM}_{2.5}$; (2) the chosen auxiliary variables improved the interpretation of the model to $\text{PM}_{2.5}$ variation. In the views of the spatial heterogeneous relationship between $\text{PM}_{2.5}$ and auxiliary variables, a local regression method, geographically weighted regression (GWR) [36], was applied to assess and describe the relationship.

For each month, observations of the training stations were used to construct the $\text{PM}_{2.5}$ estimation model, and observations from the validation stations were used to validate the accuracy of the estimated result (Figure 1). Some statistical indexes, including correlation coefficient, mean absolute error (MAE), and root-mean-square error (RMSE), were chosen to evaluate the effectiveness of the proposed model.

3.2. Effect of Economic and Social Factors on $\text{PM}_{2.5}$ Concentration

Socioeconomic data from the statistical yearbook were based on city-scale annual statistics. Hence, the derived MAPC data should be processed accordingly, which generated the city-scale annual average $\text{PM}_{2.5}$ concentration (AAPC). The logarithms of AAPC were calculated to ensure consistency with the pre-processing of Socioeconomic data.

The $\text{PM}_{2.5}$ distribution presented strong trans-regional characteristics and inevitably affected nearby regions. Global Morans' I analysis [37] was used to measure the spatial correlation of $\text{PM}_{2.5}$ concentrations. In addition, local Morans' I analysis [37] was applied to describe the spatial heterogeneity of $\text{PM}_{2.5}$ concentrations in different geographical units.

The effects of socioeconomic factors on $\text{PM}_{2.5}$ concentration in the urban scale were analyzed by a spatial panel model [38,39]:

$$\begin{aligned} \ln y_{it} &= \rho \sum_{j=1}^N w_{ij} y_{jt} + \varphi + \ln X_{it} \beta + \sum_{j=1}^N w_{ij} \ln X_{jt} \gamma + \mu_i + \eta_t + \phi_{it} \\ \phi_{it} &= \lambda \sum_{j=1}^N w_{ij} \phi_{jt} + \varepsilon_{it}, \quad \varepsilon_{it} \sim N(0, \delta^2) \end{aligned} \quad (4)$$

where i refers to city and t is the year. y_{it} is the explained variable, which is equal to AAPC of city i in year t . $\ln X_{it}$ is the explanatory variable which refers to socioeconomic factors, and β is the corresponding coefficients. μ_i is the spatial effect and η_t is the time-period effect. w_{ij} refers to elements

in the spatial weight matrix W . ρ is the spatial autoregression coefficient of dependent variables. γ denotes the spatial autocorrelation vector of explanatory variables. λ is the spatial autocorrelation coefficient of the error term.

When $\gamma = \lambda = 0$, the Equation (4) is simplified to a spatial panel lag model (SPLM):

$$\ln y_{it} = \rho \sum_{j=1}^N w_{ij} + \varphi + \ln X_{it} \beta + u_i + \eta_t + \varepsilon_{it}, \varepsilon_{it} \sim N(0, \delta^2) \quad (5)$$

When $\rho = \gamma = 0$, the Equation (4) is simplified to a spatial panel error model (SPEM):

$$\begin{aligned} \ln y_{it} &= \varphi + \ln X_{it} \beta + u_i + \eta_t + \phi_{it} \\ \phi_{it} &= \lambda \sum_{j=1}^N w_{ij} \phi_{it} + \varepsilon_{it}, \varepsilon_{it} \sim N(0, \delta^2) \end{aligned} \quad (6)$$

When $\lambda = 0$, the Equation (4) is simplified to a spatial panel Durbin model (SPDM):

$$\ln y_{it} = \rho \sum_{j=1}^N w_{ij} y_{jt} + \varphi + \ln X_{it} \beta + \sum_{j=1}^N w_{ij} \ln X_{jt} \gamma + u_i + \eta_t + \varepsilon_{it}, \varepsilon_{it} \sim N(0, \delta^2) \quad (7)$$

4. Results and Discussion

4.1. Construction of the Estimation Model

Auxiliary variables were chosen monthly according to the selection criteria in Section 3.1 (Table 2). The estimation models of all months involved MAOD, which again confirms that AOD was a good indicator of PM_{2.5} concentration. The number of other chosen auxiliary variables changes with time, indicating that although PM_{2.5} concentration was greatly affected by the climatic conditions, there was a significant temporal change in sensitivity. This validates the justifiability of the proposed assumption. Many studies [6,40] have reported that precipitation affects PM_{2.5} concentration, and the effect is more significant in the time dimension or in the large spatial range. However, in this study, we constructed an estimation model for each month, which reduces the effect in the time dimension. Next, unlike other statistical methods, GWR is a local spatial regression method—only the data within the local range participates in the model construction, thereby weakening the effect in the large spatial range. As a result, precipitation was excluded in this study. This is consistent with other studies [41–43] that build PM_{2.5} estimation models based on GWR.

Table 2. Variable selection of monthly average PM_{2.5} concentration (MAPC) estimation model for 2015–2017.

Month	Monthly average AOD data (MAOD)	AT	WS	BLH	SP
201501	√				
201502	√	√			
201503	√				√
201504	√				√
201505	√	√			
201506	√	√			
201507	√	√	√		√
201508	√		√		√
201509	√				√
201510	√	√			√
201511	√				√
201512	√	√	√		√
201601	√	√			√
201602	√			√	√

201603	✓	✓	✓	✓
201604	✓	✓		✓
201605	✓	✓		✓
201606	✓	✓		✓
201607	✓	✓	✓	✓
201608	✓			✓
201609	✓	✓		✓
201610	✓		✓	
201611	✓		✓	✓
201612	✓		✓	
201701	✓		✓	✓
201702	✓	✓		✓
201703	✓	✓	✓	
201704	✓	✓		✓
201705	✓	✓		✓
201706	✓	✓		✓
201707	✓		✓	
201708	✓		✓	
201709	✓		✓	
201710	✓		✓	✓
201711	✓		✓	✓
201712	✓		✓	✓

The proposed spatiotemporal heterogeneous model (SHM) was compared with the uniform relationship model (UM) based on multiple linear regression. The construction accuracy of the estimation model throughout the study period is shown in Figure 2. UM showed a relatively lower goodness of fit and high temporal fluctuation, with minimum and maximum values of R^2 being 0.17 and 0.67, respectively. Comparatively, SHM increased interpretation to changes in $PM_{2.5}$ concentration. Its average of R^2 (0.77) was significantly higher than that of UM (0.45), while its average of RMSE ($8.87 \mu\text{g}/\text{m}^3$) was considerably smaller than that of UM ($13.81 \mu\text{g}/\text{m}^3$). In addition, SHM demonstrated better stability. All these indicate that it is necessary to consider the spatial heterogeneity of the relationships between $PM_{2.5}$ and auxiliary variables.

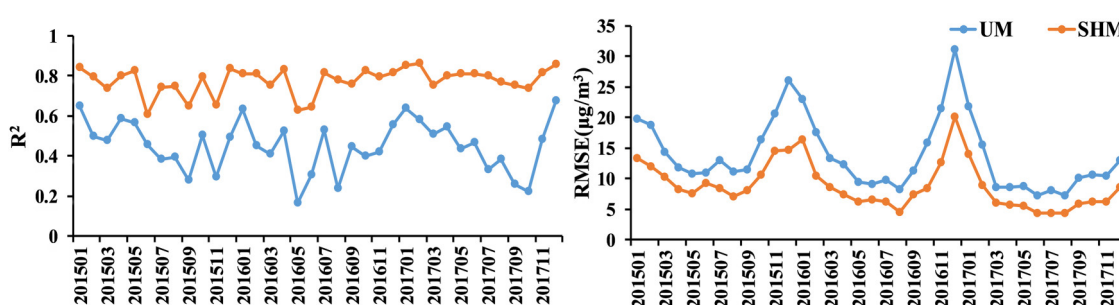


Figure 2. R^2 and root-mean-square error (RMSE) values of the derived uniform relationship model (UM) and spatiotemporal heterogeneous model (SHM) for MAPC over the study area during 2015–2017.

4.2. Accuracy Validation and Estimation Results

The validation of estimated MAPC in the study area during 2015–2017 is shown in Figure 3. R , MAE and RMSE of UM were 0.89, $11.25 \mu\text{g}/\text{m}^3$, and $15.55 \mu\text{g}/\text{m}^3$, respectively. In contrast, SHM significantly increased the estimation accuracy of MAPC, increasing the correlation coefficient by 3% and decreasing MAE and RMSE by as much as 18% and 16%, respectively. As expected, the proposed model achieved a higher estimation accuracy of AAPC than UM. The correlation coefficient of the

proposed model increased by 5%, while the MAE and RMSE decreased by as much as 19% and 17%, respectively (Figure 4). Huang et al. [44] estimated 1 km MAPC in North China from 2013–2015, with RMSE of $14.89 \mu\text{g}/\text{m}^3$. Ma et al. [45] produced China's 10 km MAPC from 2014 to 2017 using a two-stage statistical model, with R^2 ranging from 0.75 to 0.81. Wei et al. [46] estimated China's 1 km MPAC in 2016 by using a space-time random forest approach, with R^2 of 0.73 and RMSE of $14.88 \mu\text{g}/\text{m}^3$. Therefore, the overall accuracy of SHM is satisfying.

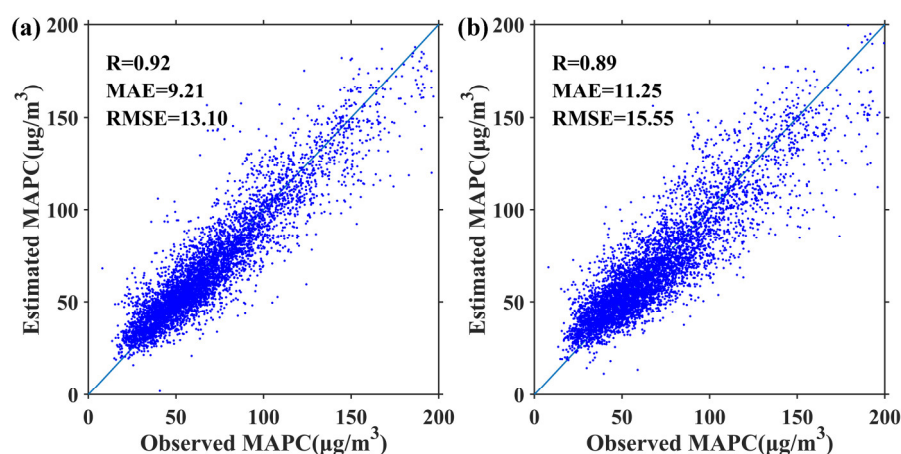


Figure 3. Scatterplots between estimated MAPC and ground observation by using SHM (a) and UM (b) over the study area during 2015–2017.

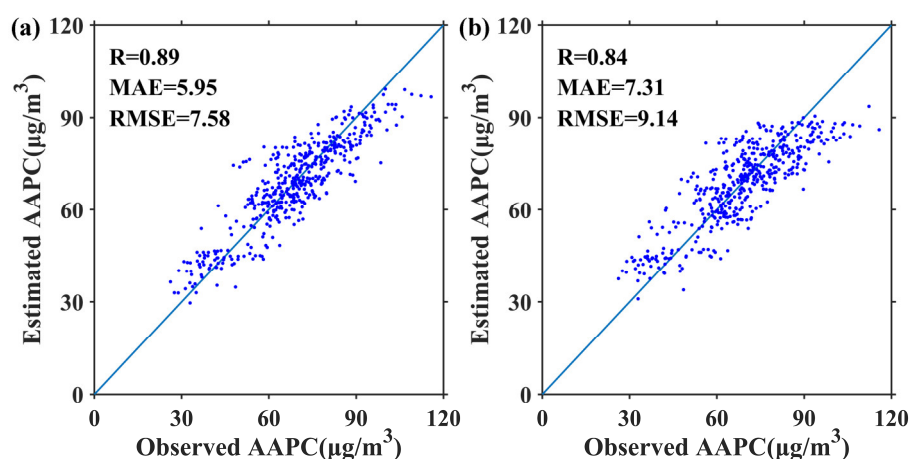


Figure 4. Scatterplots between estimated annual average $\text{PM}_{2.5}$ concentration (AAPC) and ground observation by using SHM (a) and UM (b) over the study area during 2015–2017.

Taking MAPC in 2016 as examples, their spatial distributions are shown in Figure 5. There is a significant spatiotemporal variation in $\text{PM}_{2.5}$ concentration. In terms of spatial variation, high MAPC in the southeast region of the study area from January–April was observed, whereas $\text{PM}_{2.5}$ concentration in the northwest region towards the central area was relatively higher from May–December. With regards to temporal variation, $\text{PM}_{2.5}$ concentrations in January, February, November, and December were significantly higher than those in other months. The reason behind this may be related to indoor heating and climatic conditions. Some studies have reported that the burning of biomass and fossil energy for heating in winter generated huge $\text{PM}_{2.5}$ emissions [47,48]. Dust storms, which frequently occur in North China in late winter and spring, is another major contribution that aggravates $\text{PM}_{2.5}$ concentrations [49]. The lowest average MAPC ($40.33 \mu\text{g}/\text{m}^3$) occurred in August, and the highest ($138.49 \mu\text{g}/\text{m}^3$) was in December. The AAPC in the study area during 2015–2017 is shown in Figure 6. Generally, AAPC decreased from the central areas of Shijiazhuang, Baoding, Hengshui, and Xingtai to surrounding areas, accompanied with obvious concentration characteristics. The average AAPC decreased from $77.3 \mu\text{g}/\text{m}^3$ in 2015 to $64.85 \mu\text{g}/\text{m}^3$ in 2017.

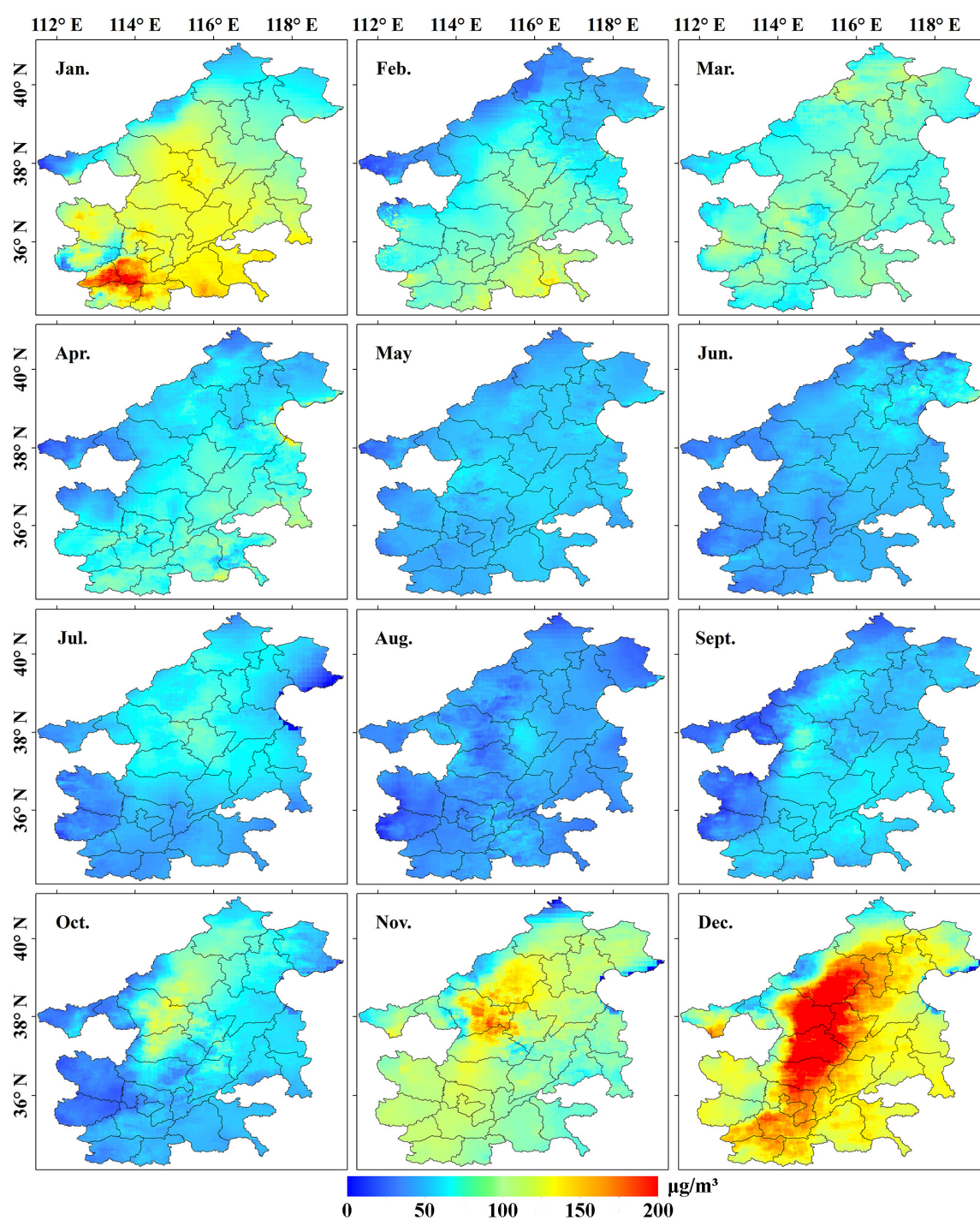


Figure 5. Spatial distribution of MAPC in each month of 2016.

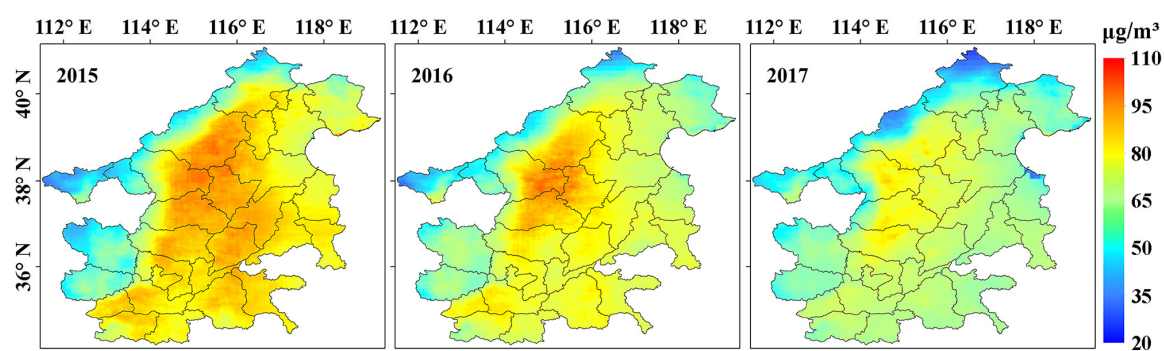


Figure 6. Spatial distribution of AAPC in 2015, 2016, and 2017.

4.3. Spatiotemporal Analysis of City-Scale PM_{2.5} Concentration

Spatiotemporal variations of city-scale AAPC in the study area are shown in Figure 7. The AAPC in Taiyuan, Yangquan, Changzhi, and Jincheng changed slightly, but AAPC in the other cities decreased year by year, especially in Hengshui, Liaocheng, Dezhou, and Jinan. This might be related to the relatively high PM_{2.5} pollution present in these cities. Nevertheless, AAPC in all cities were still higher than the national environmental air quality standard of 35 $\mu\text{g}/\text{m}^3$ (GB3095-2012), and much higher than the health standard recommended by the WHO of 10 $\mu\text{g}/\text{m}^3$. This demonstrated that more work is required to control PM_{2.5} concentrations in the study area.

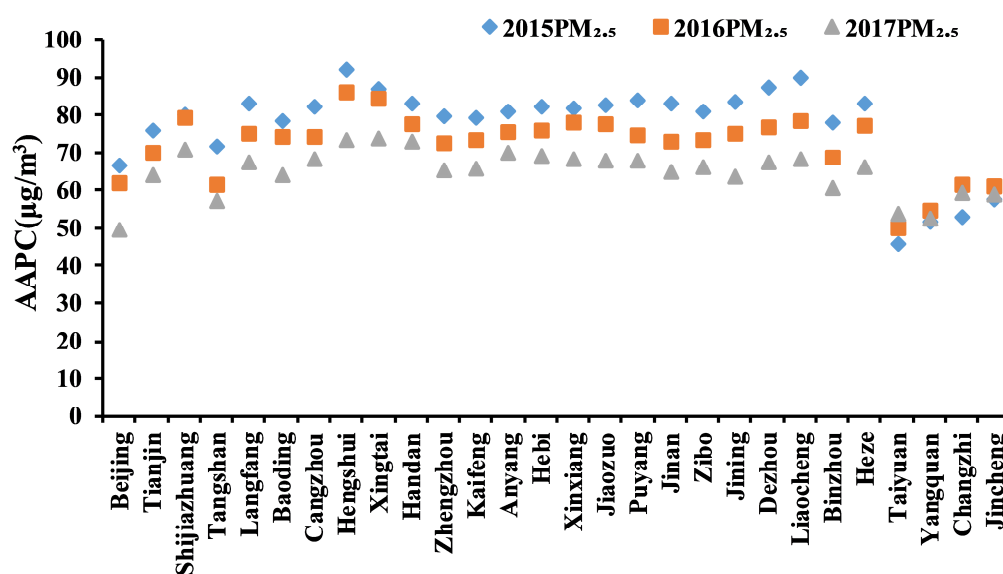


Figure 7. AAPC of 28 cities during 2015–2017.

Figure 8 shows the spatial correlation of city-scale AAPC in the study area. Global Moran's I indexes were positive during 2015–2017 and all passed the significance test of 0.05, indicating that AAPC had significant spatial positive correlation and evident spatial concentration. Moreover, the Global Moran's I decreased gradually, indicating that the concentration degree of AAPC decreased year by year.

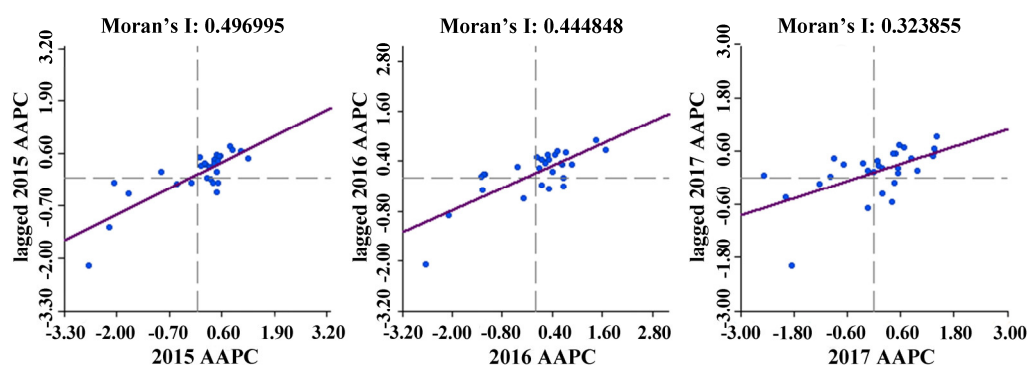


Figure 8. Global Moran's I scatterplots of AAPC of 28 cities in 2015, 2016, and 2017.

To further identify the local aggregation pattern of city-scale AAPC, the local Moran's I analysis was performed (Figure 9). The AAPC was dominated by high-high (HH) and low-low (LL) aggregation types; however, high-low (HL) or low-high (LH) types were not found. This indicated that AAPC in the study area had a local spatial positive correlation. HH-type regions, also known as the high-value aggregation region of AAPC, stably locate in the study area center, whereas the

distribution of LL-type regions is unstable. The LL-type regions were concentrated in the west of the study area during 2015–2016, but in the northeast region of the study area in 2017.

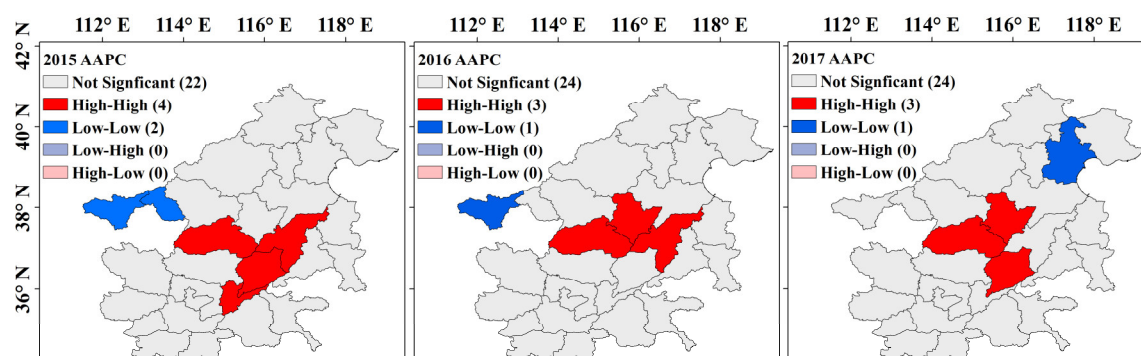


Figure 9. Local indicators of spatial association maps of city-scale AAPC for 2015, 2016, and 2017.

4.4. Effects of Socioeconomic Factors on $PM_{2.5}$ Concentration

A series of tests were required to select the optimal analysis model. Firstly, to determine whether the spatial panel model should be applied, the Lagrange Multiplier (LM), and robust LM (RLM) tests were applied to assess the spatial correlation of the errors of the classic panel model. The LM error, LM lag, and RLM error under each condition (unfixed effects, spatial fixed effects, time-period fixed effects, and spatial and time-period fixed effects) all passed the 5% significance test (Table 3), indicating a significant spatial correlation of the errors in the classic panel model. Hence, the spatial panel model should be applied. The likelihood ratio (LR) tests of spatial fixed effects and time-period fixed effects both exceeded the 1% significance level, which proved the superiority of spatial and time-period fixed effects to the spatial fixed effects or time-period fixed effects. Subsequently, a spatial panel Durbin model with spatial and time-period fixed effects was constructed to test whether it could be simplified into SPLM or SPEM (Table 4). The Hausman test was significant at the 1% level, indicating that the model with random effects was rejected; the Wald and LR tests were significant at the 1% level. Therefore, the spatial panel Durbin model could not be simplified.

Table 3. Diagnostic tests for non-spatial panel model.

Diagnostic Tests	No fixed effects (FE)	Spatial FE	Time FE	Two-Way FE
LM test spatial error	15.9629 ***	23.8827 ***	11.4793 ***	23.9171 ***
RLM test spatial error	8.4256 ***	27.7504 ***	6.4073 **	16.7844 ***
LM test spatial lag	7.6638 ***	5.0589 **	5.3875 **	13.1293 ***
RLM test spatial lag	0.1265	8.9266 ***	0.3154	5.9966 **
LR test		182.6997 ***	10.5856 **	

Note: ***, ** and * indicate significance at the 1%, 5%, and 10% levels, respectively.

Table 4. Diagnostic tests for SPDM with two-way FE.

Diagnostic Tests	Statistics
Hausman test	148.1871 ***
Wald test spatial lag	27.9485 ***
LR spatial lag	25.0216 ***
Wald test spatial error	35.8282 ***
LR spatial error	29.7859 ***

Note: ***, ** and * represent significance at the 1%, 5%, and 10% levels, respectively.

The spatial panel Durbin model with spatial and time-period fixed effects was chosen to analyze how economic and social factors influence $PM_{2.5}$ concentration. As shown in Table 5, UR has a significantly negative effect on $PM_{2.5}$ concentration, and increasing the UR of a city by 1% could decrease $PM_{2.5}$ concentration in the city by 0.78%. This is because, with the increasing demands for

people to live in a healthy environment, China has implemented stricter environmental regulations than before. Considering the spatial interaction of UR, the PM_{2.5} concentration in a city could decrease by 2.23% if the UR in the surrounding cities is increased by 1%. Our findings are different from studies before 2010 [50], which suggested that UR has a positive effect on PM_{2.5} concentration. The reason behind this is that after China made carbon emission reduction commitments at the 2009 Copenhagen Climate Conference, the government, enterprises, and society have been vigorously promoting ecological sustainability, which effectively curbed the aggravation of air pollution, and reduced PM_{2.5} concentration.

Table 5. Estimation results of SPDM with two-way FE.

	Coefficient	t Value		Coefficient	t Value
<i>lnPD</i>	−0.0141	−0.5963	<i>W*lnPD</i>	−0.0243	−0.5542
<i>lnPGRP</i>	0.7351 *	0.8572	<i>W*lnPGRP</i>	2.7496 *	1.7305
<i>(lnPGRP)²</i>	−0.0332 *	−0.8595	<i>W*(lnPGRP)²</i>	−0.1359 *	−1.7796
<i>lnUR</i>	−0.7856 **	−2.1325	<i>W*lnUR</i>	−2.2324 ***	−3.0512
<i>lnPSIGDP</i>	−0.1035	−1.1761	<i>W*lnPSIGDP</i>	0.3455	1.8127
<i>lnISDE</i>	0.0095	0.7338	<i>W*lnISDE</i>	0.0432 *	1.9087
<i>lnNIEDS</i>	0.1491 *	1.7273	<i>W*lnIEDS</i>	0.6736 ***	2.6974
			<i>W*dep.var.</i>	0.6337 ***	7.6980

Note: ***, ** and * represent significance at the 1%, 5% and 10% levels, respectively.

The coefficients of *lnPGRP* and *(lnPGRP)²* were significantly positive and negative, respectively, indicating the existence of an inverted U-shaped environmental Kuznets curve (EKC) of PM_{2.5} concentration in the study area. With the increase of the per capita income level, the study area experienced a process of pollution first and then treatment, resulting in the PM_{2.5} concentration first increasing and then decreasing, which is consistent with some existing research [51–53]. Although most cities in the study area except for Beijing, Tianjin, and Qinhuaangdao are still in the stage of industrialization [54] and have a secondary industry-dominated structure, some cities shut down many small-sized, high-pollution, and high-energy-consumption enterprises in order to meet environmental quality requirements, and reached the peak of pollution ahead of schedule at the cost of low and medium economic growth. This is further demonstrated by the insignificant coefficient of PSIGDP.

Nevertheless, NIEDS has a significant positive effect on PM_{2.5} concentrations. PM_{2.5} concentrations in cities may increase by 0.15% and adjacent areas by 0.67% when NIEDS is increased by 1%. This is related to the fact that many NIEDS are resource- and energy-consuming enterprises. For example, the Hebei Iron and Steel Group is an ultra-large iron and steel group that ranks as the first in China and the second in the world in terms of crude steel output. Such enterprises provide important support for local employment and economic development. Given the path-dependence of their development, it is difficult to carry out energy saving and emission reduction measures immediately and thoroughly [55]. These enterprises will generate a large amount of dust pollution during production activities. Accordingly, the PM_{2.5} concentration of a city is increased 0.043% when the ISDE of adjacent cities is increased by 1%.

In addition to the above socioeconomic factors, the PM_{2.5} concentration of a city was also influenced by those in surrounding cities. The coefficient of the spatial lag term of PM_{2.5} concentration was 0.6337 and passed the 1% significance test, which was mainly due to the transmission and diffusion of PM_{2.5}. Wang et al. [56] also reported that the contribution rate of foreign sources to PM_{2.5} concentrations in the Beijing–Tianjin–Hebei region was 23.4%.

To further identify the influence of different social factors, we calculated the direct, indirect, and total effects of socioeconomic factors on PM_{2.5} concentration (Table 6). Among seven factors, the total effect of *lnPGRP*, *(lnPGRP)²*, *lnUR*, *lnISDE*, and *lnNIEDS* passed the significance test, indicating that these five factors influenced the spatiotemporal distribution of PM_{2.5} concentration in the study area. The order of the degree of influence for these five factors was: *lnPGRP* > *lnUR* > *lnNIEDS* > *(lnPGRP)²* > *lnISDE*. The other factors may not significantly influence PM_{2.5} concentration. To be specific, *lnPGRP*

and $\ln UR$ are primary factors that influenced $PM_{2.5}$ concentration, and the $\ln PGRP$, $\ln UR$, and $\ln NIEDS$ have spillover effects on the $PM_{2.5}$ concentration in surrounding cities.

Table 6. Decomposed spatial effects of SPDM with two-way FE.

	Direct Effects	<i>t</i> Value	Indirect Effects	<i>t</i> Value	Total Effects	<i>t</i> Value
$\ln PD$	−0.0219	−0.6611	−0.0798	−0.6100	−0.1017	−0.6452
$\ln PGRP$	1.6783 *	1.4878	8.2446 *	1.7204	9.9229 *	1.7623
$(\ln PGRP)^2$	−0.0790 *	−1.5492	−0.4014 *	−1.8354	−0.4804 *	−1.8706
$\ln UR$	−1.5655 ***	−3.0675	−6.8348 ***	−2.9502	−8.4003 ***	−3.0936
$\ln PSIGDP$	−0.0313	−0.2692	0.6839	1.2956	0.6527	1.0645
$\ln ISDE$	0.0234	1.3370	0.1248 *	1.7119	0.1482 *	1.7148
$\ln NIEDS$	0.3638 **	2.1617	1.8965 **	2.4697	2.2603 **	2.4722

Note: ***, ** and * represent significance at the 1%, 5%, and 10% levels, respectively.

5. Conclusions

This study investigated the effects of socioeconomic factors on the spatiotemporal distribution of $PM_{2.5}$ in Beijing–Tianjin–Hebei and surrounding areas during 2015–2017. First, an estimation model considering spatiotemporal heterogeneous relationships was developed to depict the spatiotemporal pattern of $PM_{2.5}$ concentration in the study area. Then, on the basis of analyzing the spatiotemporal evolution of $PM_{2.5}$ concentration, a spatial panel Dubin model was applied to determine how socioeconomic factors affect $PM_{2.5}$ concentration. Major conclusions of this research include:

1. There is a significant spatiotemporal heterogeneous relationship between $PM_{2.5}$ and the chosen auxiliary variables. The developed model can well estimate the spatial distribution of $PM_{2.5}$ concentration in the study area, with MAE and RMSE of $9.21 \mu\text{g}/\text{m}^3$ and $13.1 \mu\text{g}/\text{m}^3$, respectively.
2. $PM_{2.5}$ concentration in the study area showed significant spatial and temporal changes. Although $PM_{2.5}$ concentration has decreased year by year, it was still higher than the national quality standard. Thus, further reduction in $PM_{2.5}$ concentration remains a huge challenge.
3. PGRP, UR, and NIEDS were the key factors influencing the spatiotemporal distribution of $PM_{2.5}$ concentration in the study area. Specially, there was an inverted U-shaped relationship between PGRP and $PM_{2.5}$ concentrations. In addition, the increase of UR in a city will reduce $PM_{2.5}$ concentration not only in its own city but in neighboring cities, while the increase of NIEDS of a city will exacerbate $PM_{2.5}$ concentration in its own city and neighboring cities.

Author Contributions: Methodology and formal analysis: W.W. and L.Z.; data curation and visualization: J.Z. and M.Q.; conceptualization, methodology, writing—original draft, and supervision: F.C. All authors have read and agreed to the published version of the manuscript.

Funding: This work was supported by the Natural Science Foundation of China (41401503), the Training Plan for University Young Key Teacher by Henan Province, the Scientific Research Start-up Funding of the Program Supporting Special Talent Zone (Henan University), and the Scientific Promotion Funding of the Prioritized Academic Discipline (Geography, Henan University).

Conflicts of Interest: The authors declare no conflict of interest.

References

1. Xu, Q. Abrupt change of the mid-summer climate in central east China by the influence of atmospheric pollution. *Atmos. Environ.* **2001**, *35*, 5029–5040, doi:10.1016/S1352-2310(01)00315-6.
2. Borrego, C.; Martins, H.; Tchepel, O.; Salmim, L.; Monteiro, A.; Miranda, A. How urban structure can affect city sustainability from an air quality perspective. *Environ. Model. Softw.* **2006**, *21*, 461–467, doi:10.1016/j.envsoft.2004.07.009.

3. Fang, B.; Zhang, L.; Zeng, H.; Liu, J.; Yang, Z.; Wang, H.; Wang, Q.; Wang, M.; Wang, P.M. 2.5-Bound Polycyclic Aromatic Hydrocarbons: Sources and Health Risk during Non-Heating and Heating Periods (Tangshan, China). *Int. J. Environ. Res. Public Health* **2020**, *17*, 483, doi:10.3390/ijerph17020483.
4. He, L.; Liu, Y.; Zhou, H.; He, L.; Liu, Y.; He, P.; Zhou, H. Relationship between Air Pollution and Urban Forms: Evidence from Prefecture-Level Cities of the Yangtze River Basin. *Int. J. Environ. Res. Public Health* **2019**, *16*, 3459, doi:10.3390/ijerph16183459.
5. Kuehn, B.M. WHO: More Than 7 Million Air Pollution Deaths Each Year. *JAMA* **2014**, *311*, 1486, doi:10.1001/jama.2014.4031.
6. Burnett, R.; Chen, H.; Szyszkowicz, M.; Fann, N.; Hubbell, B.; Pope, C.A.; Apte, J.S.; Brauer, M.; Cohen, A.; Weichenthal, S.; et al. Global estimates of mortality associated with long-term exposure to outdoor fine particulate matter. *Proc. Natl. Acad. Sci. USA* **2018**, *115*, 9592–9597.
7. Wang, Z.; Yang, L. Delinking indicators on regional industry development and carbon emissions: Beijing–Tianjin–Hebei economic band case. *Ecol. Indic.* **2015**, *48*, 41–48, doi:10.1016/j.ecolind.2014.07.035.
8. Janssen, S.; Dumont, G.; Fierens, F.; Mensink, C. Spatial interpolation of air pollution measurements using CORINE land cover data. *Atmos. Environ.* **2008**, *42*, 4884–4903, doi:10.1016/j.atmosenv.2008.02.043.
9. Lee, S.-J.; Serre, M.; Van Donkelaar, A.; Martin, R.V.; Burnett, R.T.; Jerrett, M. Comparison of Geostatistical Interpolation and Remote Sensing Techniques for Estimating Long-Term Exposure to Ambient PM_{2.5} Concentrations across the Continental United States. *Environ. Health Perspect.* **2012**, *120*, 1727–1732, doi:10.1289/ehp.1205006.
10. Van Donkelaar, A.; Martin, R.V.; Park, R. Estimating ground-level PM_{2.5} using aerosol optical depth determined from satellite remote sensing. *J. Geophys. Res. Space Phys.* **2006**, *111*, 21201, doi:10.1029/2005jd006996.
11. Van Donkelaar, A.; Martin, R.V.; Brauer, M.; Kahn, R.; Levy, R.C.; Verduzco, C.; Villeneuve, P.J. Global Estimates of Ambient Fine Particulate Matter Concentrations from Satellite-Based Aerosol Optical Depth: Development and Application. *Environ. Health Perspect.* **2010**, *118*, 847–855, doi:10.1289/ehp.0901623.
12. Robichaud, A.; Menard, R. Multi-year objective analyses of warm season ground-level ozone and PM_{2.5} over North America using real-time observations and Canadian operational air quality models. *Atmos. Chem. Phys. Discuss.* **2014**, *14*, 1769–1800, doi:10.5194/acp-14-1769-2014.
13. Liu, Y.; Franklin, M.; Kahn, R.; Koutrakis, P. Using aerosol optical thickness to predict ground-level PM_{2.5} concentrations in the St. Louis area: A comparison between MISR and MODIS. *Remote Sens. Environ.* **2007**, *107*, 33–44, doi:10.1016/j.rse.2006.05.022.
14. Paciorek, C.; Liu, Y.; Moreno-Macias, H.; Kondragunta, S. Spatiotemporal Associations between GOES Aerosol Optical Depth Retrievals and Ground-Level PM_{2.5}. *Environ. Sci. Technol.* **2008**, *42*, 5800–5806, doi:10.1021/es703181j.
15. Liu, Y.; Paciorek, C.; Koutrakis, P. Estimating Regional Spatial and Temporal Variability of PM_{2.5} Concentrations Using Satellite Data, Meteorology, and Land Use Information. *Environ. Health Perspect.* **2009**, *117*, 886–892, doi:10.1289/ehp.0800123.
16. Lee, H.J.; Liu, Y.; Coull, B.A.; Schwartz, J.; Koutrakis, P. A novel calibration approach of MODIS AOD data to predict PM_{2.5} concentrations. *Atmos. Chem. Phys. Discuss.* **2011**, *11*, 7991–8002, doi:10.5194/acp-11-7991-2011.
17. Xie, Y.; Wang, Y.; Zhang, K.; Dong, W.; Lv, B.; Bai, Y. Daily Estimation of Ground-Level PM_{2.5} Concentrations over Beijing Using 3 km Resolution MODIS AOD. *Environ. Sci. Technol.* **2015**, *49*, 12280–12288, doi:10.1021/acs.est.5b01413.
18. Ma, Z.; Liu, Y.; Zhao, Q.; Liu, M.; Zhou, Y.; Bi, J. Satellite-derived high resolution PM_{2.5} concentrations in Yangtze River Delta Region of China using improved linear mixed effects model. *Atmos. Environ.* **2016**, *133*, 156–164, doi:10.1016/j.atmosenv.2016.03.040.
19. Wang, J.; Ogawa, S. Effects of Meteorological Conditions on PM_{2.5} Concentrations in Nagasaki, Japan. *Int. J. Environ. Res. Public Health* **2015**, *12*, 9089–9101, doi:10.3390/ijerph120809089.
20. Guo, J.; Xia, F.; Zhang, Y.; Liu, H.; Li, J.; Lou, M.; He, J.; Yan, Y.; Wang, F.; Min, M.; et al. Impact of diurnal variability and meteorological factors on the PM_{2.5}–AOD relationship: Implications for PM_{2.5} remote sensing. *Environ. Pollut.* **2017**, *221*, 94–104, doi:10.1016/j.envpol.2016.11.043.
21. DeGaetano, A.T.; Doherty, O.M. Temporal, spatial and meteorological variations in hourly PM_{2.5} concentration extremes in New York City. *Atmos. Environ.* **2004**, *38*, 1547–1558, doi:10.1016/j.atmosenv.2003.12.020.

22. Zhang, Z.; Zhang, X.; Gong, D.; Quan, W.; Zhao, X.; Ma, Z.; Kim, S.-J. Evolution of surface O₃ and PM_{2.5} concentrations and their relationships with meteorological conditions over the last decade in Beijing. *Atmos. Environ.* **2015**, *108*, 67–75, doi:10.1016/j.atmosenv.2015.02.071.
23. Hao, Y.; Liu, Y.-M. The influential factors of urban PM_{2.5} concentrations in China: A spatial econometric analysis. *J. Clean. Prod.* **2016**, *112*, 1443–1453, doi:10.1016/j.jclepro.2015.05.005.
24. Wang, S.; Zhou, C.; Wang, Z.; Feng, K.; Hubacek, K. The characteristics and drivers of fine particulate matter (PM_{2.5}) distribution in China. *J. Clean. Prod.* **2017**, *142*, 1800–1809, doi:10.1016/j.jclepro.2016.11.104.
25. Wang, Z.; Fang, C.-L. Spatial-temporal characteristics and determinants of PM_{2.5} in the Bohai Rim Urban Agglomeration. *Chemosphere* **2016**, *148*, 148–162, doi:10.1016/j.chemosphere.2015.12.118.
26. Liu, Q.; Wang, S.; Zhang, W.; Li, J.; Dong, G. The effect of natural and anthropogenic factors on PM_{2.5}: Empirical evidence from Chinese cities with different income levels. *Sci. Total Environ.* **2019**, *653*, 157–167, doi:10.1016/j.scitotenv.2018.10.367.
27. Zhou, C.; Chen, J.; Wang, S. Examining the effects of socioeconomic development on fine particulate matter (PM_{2.5}) in China's cities using spatial regression and the geographical detector technique. *Sci. Total Environ.* **2017**, *619*, 436–445, doi:10.1016/j.scitotenv.2017.11.124.
28. Guan, D.; Su, X.; Zhang, Y.; Peters, G.; Liu, Z.; Lei, Y.; He, K. The socioeconomic drivers of China's primary PM_{2.5} emissions. *Environ. Res. Lett.* **2014**, *9*, 024010, doi:10.1088/1748-9326/9/2/024010.
29. Lu, D.; Xu, J.; Yang, D.; Zhao, J. Spatio-temporal variation and influence factors of PM_{2.5} concentrations in China from 1998 to 2014. *Atmos. Pollut. Res.* **2017**, *8*, 1151–1159, doi:10.1016/j.apr.2017.05.005.
30. Cheng, Z.; Li, L.; Liu, J. Identifying the spatial effects and driving factors of urban PM_{2.5} pollution in China. *Ecol. Indic.* **2017**, *82*, 61–75, doi:10.1016/j.ecolind.2017.06.043.
31. Han, L.; Zhou, W.; Li, W. Fine particulate (PM_{2.5}) dynamics during rapid urbanization in Beijing, 1973–2013. *Sci. Rep.* **2016**, *6*, 23604, doi:10.1038/srep23604.
32. Lin, G.; Fu, J.; Jiang, D.; Hu, W.; Dong, D.; Huang, Y.; Zhao, M. Spatio-Temporal Variation of PM_{2.5} Concentrations and Their Relationship with Geographic and Socioeconomic Factors in China. *Int. J. Environ. Res. Public Health* **2013**, *11*, 173–186, doi:10.3390/ijerph110100173.
33. Du, Y.; Wan, Q.; Liu, H.; Liu, H.; Kapsar, K.; Peng, J.; Kasper, K. How does urbanization influence PM_{2.5} concentrations? Perspective of spillover effect of multi-dimensional urbanization impact. *J. Clean. Prod.* **2019**, *220*, 974–983, doi:10.1016/j.jclepro.2019.02.222.
34. Tai, A.P.K.; Mickley, L.J.; Jacob, D.J. Correlations between fine particulate matter (PM_{2.5}) and meteorological variables in the United States: Implications for the sensitivity of PM_{2.5} to climate change. *Atmos. Environ.* **2010**, *44*, 3976–3984, doi:10.1016/j.atmosenv.2010.06.060.
35. Wang, L.; Zhang, N.; Liu, Z.; Sun, Y.; Ji, D.; Wang, Y. The Influence of Climate Factors, Meteorological Conditions, and Boundary-Layer Structure on Severe Haze Pollution in the Beijing-Tianjin-Hebei Region during January 2013. *Adv. Meteorol.* **2014**, *2014*, 1–14, doi:10.1155/2014/685971.
36. Brunson, C.; Fotheringham, S.; Charlton, M. Geographically Weighted Regression. *J. R. Stat. Soc. Ser. D Stat.* **1998**, *47*, 431–443, doi:10.1111/1467-9884.00145.
37. Bivand, R.; Müller, W.; Reder, M. Power calculations for global and local Moran's. *Comput. Stat. Data Anal.* **2009**, *53*, 2859–2872, doi:10.1016/j.csda.2008.07.021.
38. Elhorst, J.P. Specification and Estimation of Spatial Panel Data Models. *Int. Reg. Sci. Rev.* **2003**, *26*, 244–268, doi:10.1177/0160017603253791.
39. LeSage, J.; Pace, R.K. *Introduction to Spatial Econometrics*; Chapman and Hall/CRC: London, UK, 2009.
40. Guo, L.-C.; Zhang, Y.; Lin, H.; Zeng, W.; Liu, T.; Xiao, J.; Rutherford, S.; You, J.; Ma, W. The washout effects of rainfall on atmospheric particulate pollution in two Chinese cities. *Environ. Pollut.* **2016**, *215*, 195–202, doi:10.1016/j.envpol.2016.05.003.
41. Hu, X.; Waller, L.A.; Al-Hamdan, M.Z.; Crosson, W.L.; Estes, M.G., Jr.; Estes, S.M.; Quattrochi, D.; Sarnat, J.A.; Liu, Y. Estimating ground-level PM_{2.5} concentrations in the southeastern U.S. using geographically weighted regression. *Environ. Res.* **2013**, *121*, 1–10, doi:10.1016/j.envres.2012.11.003.
42. You, W.; Zang, Z.; Zhang, L.; Li, Y.; Pan, X.; Wang, W. National-Scale Estimates of Ground-Level PM_{2.5} Concentration in China Using Geographically Weighted Regression Based on 3 km Resolution MODIS AOD. *Remote. Sens.* **2016**, *8*, 184, doi:10.3390/rs8030184.
43. Jiang, M.; Sun, W.; Yang, G.; Zhang, D. Modelling Seasonal GWR of Daily PM_{2.5} with Proper Auxiliary Variables for the Yangtze River Delta. *Remote. Sens.* **2017**, *9*, 346, doi:10.3390/rs9040346.

44. Huang, K.; Xiao, Q.; Meng, X.; Geng, G.; Wang, Y.; Lyapustin, A.; Gu, D.-F.; Liu, Y. Predicting monthly high-resolution PM_{2.5} concentrations with random forest model in the North China Plain. *Environ. Pollut.* **2018**, *242*, 675–683, doi:10.1016/j.envpol.2018.07.016.
45. Ma, Z.; Liu, R.; Liu, Y.; Bi, J. Effects of air pollution control policies on PM_{2.5} pollution improvement in China from 2005 to 2017: A satellite-based perspective. *Atmos. Chem. Phys. Discuss.* **2019**, *19*, 6861–6877, doi:10.5194/acp-19-6861-2019.
46. Wei, J.; Huang, W.; Li, Z.; Xue, W.; Peng, Y.; Sun, L.; Cribb, M.C. Estimating 1-km-resolution PM_{2.5} concentrations across China using the space-time random forest approach. *Remote. Sens. Environ.* **2019**, *231*, 111221, doi:10.1016/j.rse.2019.111221.
47. Chai, F.; Gao, J.; Chen, Z.; Wang, S.; Zhang, Y.; Zhang, J.; Zhang, H.; Yun, Y.; Ren, C. Spatial and temporal variation of particulate matter and gaseous pollutants in 26 cities in China. *J. Environ. Sci.* **2014**, *26*, 75–82, doi:10.1016/s1001-0742(13)60383-6.
48. Yang, L.; Cheng, S.; Wang, X.; Nie, W.; Xu, P.; Gao, X.; Yuan, C.; Wang, W. Source identification and health impact of PM_{2.5} in a heavily polluted urban atmosphere in China. *Atmos. Environ.* **2013**, *75*, 265–269, doi:10.1016/j.atmosenv.2013.04.058.
49. Lin, C.; Li, Y.; Yuan, Z.; Lau, A.K.; Li, C.; Fung, J.C.H. Using satellite remote sensing data to estimate the high-resolution distribution of ground-level PM_{2.5}. *Remote. Sens. Environ.* **2015**, *156*, 117–128, doi:10.1016/j.rse.2014.09.015.
50. Du, Y.; Sun, T.; Peng, J.; Fang, K.; Liu, Y.; Yang, Y.; Wang, Y. Direct and spillover effects of urbanization on PM_{2.5} concentrations in China's top three urban agglomerations. *J. Clean. Prod.* **2018**, *190*, 72–83, doi:10.1016/j.jclepro.2018.03.290.
51. Ma, Y.-R.; Ji, Q.; Fan, Y. Spatial linkage analysis of the impact of regional economic activities on PM 2.5 pollution in China. *J. Clean. Prod.* **2016**, *139*, 1157–1167, doi:10.1016/j.jclepro.2016.08.152.
52. Dong, K.; Sun, R.-J.; Dong, C.; Li, H.; Zeng, X.; Ni, G. Environmental Kuznets curve for PM_{2.5} emissions in Beijing, China: What role can natural gas consumption play? *Ecol. Indic.* **2018**, *93*, 591–601, doi:10.1016/j.ecolind.2018.05.045.
53. Álvarez-Herranz, A.; Balsalobre-Lorente, D.; Shahbaz, M.; Cantos, J.M. Energy innovation and renewable energy consumption in the correction of air pollution levels. *Energy Policy* **2017**, *105*, 386–397, doi:10.1016/j.enpol.2017.03.009.
54. Ding, Y.; Zhang, M.; Chen, S.; Wang, W.; Nie, R. The environmental Kuznets curve for PM_{2.5} pollution in Beijing-Tianjin-Hebei region of China: A spatial panel data approach. *J. Clean. Prod.* **2019**, *220*, 984–994, doi:10.1016/j.jclepro.2019.02.229.
55. Wang, K.; Tian, H.; Hua, S.; Zhu, C.; Gao, J.; Xue, Y.; Hao, J.; Wang, Y.; Zhou, J. A comprehensive emission inventory of multiple air pollutants from iron and steel industry in China: Temporal trends and spatial variation characteristics. *Sci. Total Environ.* **2016**, *559*, 7–14, doi:10.1016/j.scitotenv.2016.03.125.
56. Wang, X.; Lang, J.; Cheng, S.; Chen, G.; Liu, X. Study on transportation of PM_{2.5} in Beijing-Tianjin-Hebei (BTH) and its surrounding area. *China Environ. Sci.* **2016**, *36*, 3211–3217.

